Light-emitting current of electrically driven single-photon sources

David M.-T. Kuo
Department of Electrical Engineering, National Central University, Chung-Li, Taiwan, 320, Republic of China
(Received 19 May 2006; published 18 September 2006)

The time-dependent tunneling current arising from the electron-hole recombination of the exciton state is theoretically studied using the nonequilibrium Green's function technique and the Anderson model with two energy levels. Charge conservation and gauge invariance are satisfied in the tunneling current. Apart from the classical capacitive charging and discharging behavior, tunneling oscillations are superimposed on the tunneling current for applied rectangular pulse voltages.

DOI: 10.1103/PhysRevB.74.115311 PACS number(s): 73.63.Kv, 73.21.La, 73.23.Hk, 78.67.Hc

I. INTRODUCTION

Recently, much effort has been devoted to the study of single-photon sources (SPSs) made from quantum dots (QDs), which have potential applications in quantum cryptography and quantum computing.[1–3] The second-order correlation function of light emitted from such devices must be measured to determine their functionality as SPSs, that is, the light source antibunching feature must be examined. The antibunching features of SPSs were demonstrated in Refs. 1 and 2, where electrons and holes in the QD are excited by optical pumping. Nevertheless, only a few experiments have employed electrical pumping to demonstrate the antibunching behavior of SPSs. From a practical point of view, it is more efficient to use electrically driven SPSs. A prototype SPS made from individual QDs embedded in a semiconductor *p-n* junction was suggested by Imamoglu and Yamamoto.[4] In addition to antibunching, enhancing the spontaneous emission rate is necessary, because it is crucial to SPS performance.

For small-size QDs, the strong three-dimensional confinement effect creates large energy separations among the low-lying confined levels. Consequently, it is possible to inject electrons and holes into the corresponding ground-state energy levels of a single QD and generate photons via electron-hole recombination in the exciton, positive or negative trion, or biexciton states in the QD. To fabricate a single nanometer-sized QD at a specific location is one of the most challenging processes in the realization of electrically driven SPSs. Self-assembled quantum dots (SAQDs) combined with a selective formation method may overcome this difficulty.[5] Even though some theoretical studies have been devoted to electrically driven SPS devices,[6–8] the dynamic properties of an electrically driven SPS are still not clear. In Ref. 4, the Monte Carlo method was used to simulate junction dynamics, where the time-dependent junction voltage is calculated. Other studies emphasized steady state characteristics such as the exciton-assisted tunneling current,[6] the Purcell effect on the tunneling current,[7] and electrode effects on the exciton complexes.[8]

The main purpose of this study is to investigate the time-dependent tunneling current (or spontaneous emission rate) arising from electron-hole recombination of the exciton state by using the nonequilibrium Green's function technique,[9–11] which has been applied to several different systems.[12–15] This study attempts to clarify how the carrier tunneling process, applied modulation voltage, and temperature influence the spontaneous emission rate in an electrically driven SPS. The schematic band diagram describing the studied system is shown in Fig. 1. Only the ground states of the conduction and valence bands of the QD are considered. The energy level of E_2 is 20 meV below the Fermi energy level of the left electrode, $E_{F,e}$=50 meV. On the other hand, the exciton state denoted by E_{ex} is 15 meV above the Fermi energy of the right electrode, $E_{F,h}$=50 meV. $\Gamma_{2(1)}$ denotes the tunneling rate from the QD to the left (right) electrode. Emitted photons will be observed when the periodic square bumplike modulation $v(t)$ added to the right electrode injects holes into the exciton resonant level.

II. HAMILTONIAN

The Anderson model with two energy levels in terms of the electron picture is used to describe the system as shown in Fig. 1,

$$H = \sum_k \epsilon_{k,L} a_k^\dagger a_k + \sum_k \epsilon_{k,R} b_k^\dagger b_k + \sum_{\ell=1,2} \epsilon_\ell d_\ell^\dagger d_\ell + \lambda_{12} d_1^\dagger d_2 + \lambda_{21}^* d_2^\dagger d_1 + \sum_{k,1} t_{k,1} b_k^\dagger d_1 + \text{H.c.} + \sum_{k,2} t_{k,2}^\dagger a_k^\dagger d_2 + \text{H.c.} \quad (1)$$

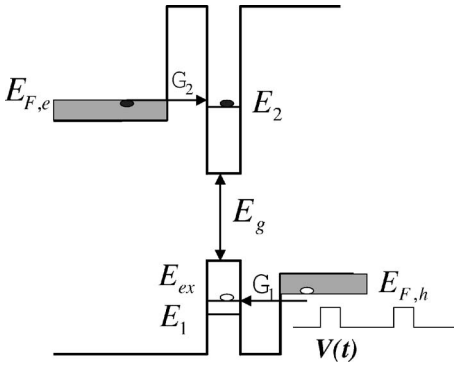

FIG. 1. The schematic band diagram for the single quantum dot embedded in a *p-i-n* junction. The ground-state energy level of electrons is 20 meV below the Fermi energy of the left electrode, and the exciton resonant state of holes is 15 meV above the Fermi energy of the right electrode. The periodic square bumplike modulation $v(t)$ supplies holes into the quantum dot.

where $a_k^\dagger$ (a_k) and $b_k^\dagger$ (b_k) create (destroy) an electron of momentum k in the left and right system electrodes, respectively. The free electron model is used in the electrodes, in which electrons have frequency-dependent energies $\epsilon_{k,L}=\epsilon_k-\omega/2$ and $\epsilon_{k,R}=\epsilon_k+\omega/2+v(t)$. The time-dependent modulation $v(t)$ denotes the time-dependent applied voltage in the right electrode. $d_\ell^\dagger$ (d_ℓ) creates (destroys) an electron inside the QD with orbital energy $\epsilon_\ell=E_\ell-(-1)^\ell\omega/2$. In this study $\ell=1$ and 2 represent, respectively, the ground states of the valence and conduction bands of individual QDs. The fourth and fifth terms describe the coupling of the QD with an electromagnetic field of frequency ω. $\lambda=-\mu_r\mathcal{E}$ is the Rabi frequency, where $\mu_r=\langle 2|r|1\rangle$ is the matrix element for the optical transition and $\mathcal{E}$ is the electric field per photon. $t_{k,\ell}$ describes the coupling between the band states of electrodes and energy levels of the QD. Note that a unitary transformation $S(t)=\exp\{i\omega t/2[\Sigma_k(b_k^\dagger b_k-a_k^\dagger a_k)+d_1^\dagger d_1-d_2^\dagger d_2]\}$, has been used to obtain Eq. (1) via

$$H=S^{-1}H(t)S-iS^{-1}\frac{\partial}{\partial t}S.$$

For small semiconductor QDs, the particle correlation is strong. This indicates that the intralevel Coulomb interactions of the QD, U_{11} and U_{22}, cannot be ignored. In order to simplify this problem, it is assumed that the regime of the applied voltage cannot overcome the charging energies U_{11} and U_{22}.[8] To investigate the exciton-assisted process,[6,8] the interlevel Coulomb interaction U_{12} is taken into account in Eq. (1),

$$H_U=U_{12}d_1^\dagger d_1 d_2^\dagger d_2, \tag{2}$$

which is invariant under unitary transformation.

III. FORMALISM

Although the spontaneous emission process of photons is a quantum effect of the electromagnetic field,[8] the electromagnetic field is still treated as a semiclassical field in Eq. (1). The approach detailed in Ref. 11 is employed to study the spontaneous emission process of photons. The optical susceptibility of QDs not only provides the absorption coefficient and the refractive index, but also determines the spontaneous emission rate.[11] Therefore, the optical susceptibility of individual QDs is calculated using the lesser Green's function defined as $G_{\ell,j}^<(t,t')=i\langle d_\ell^\dagger(t')d_j(t)\rangle$. Based on Keldysh's equation, we have

$$G_{\ell,j}^<(t,t)=\int dt_1\int dt_2 G_{\ell,n}^r(t,t_1)\Sigma_{n,m}^<(t_1,t_2)G_{m,j}^a(t_2,t), \tag{3}$$

where $\Sigma_{n,m}^<$, $G_{\ell,n}^r$, and $G_{m,j}^a$ are the lesser self-energy, the retarded Green's function, and the advanced Green's function, respectively. The Einstein summation index is used in Eq. (3). The spontaneous emission rate will be suppressed if the tunneling rates Γ_2 and Γ_1 are smaller than the spontaneous emission rate R_{eh}. The detailed expression of R_{eh} is given later. To avoid the suppression of the spontaneous emission rate, the device shown in Fig. 1 favors the condition of $\Gamma_2>\Gamma_1\gg R_{eh}$ or $\Gamma_1>\Gamma_2\gg R_{eh}$ to function as a light-emitting source. The condition of $\Gamma_2>\Gamma_1\gg R_{eh},\lambda_{\ell,j}$ will be regarded as a small parameter in the comparison with $t_{k,\ell}$. Consequently, the lesser self-energy of Eq. (3) is mainly attributed to tunneling:

$$\Sigma_{\ell,\ell}^<(t,t')=i\int\frac{d\epsilon}{2\pi}\Gamma_\ell f_\ell(\epsilon)e^{-i\epsilon(t-t')}, \tag{4}$$

where the tunneling rates are $\Gamma_\ell=\Sigma_k t_{k,\ell}t_{k,\ell}^*\delta(\epsilon-\epsilon_k)$, and $f_\ell(\epsilon)=1/(e^{\epsilon-\mu_{F,\ell}}-1)$ is the Fermi distribution function of the electrodes, in which the chemical potential is given by $\mu_{F,\ell}=E_{F,\ell}-(1)^\ell\omega/2$. It is worth noting that energy-independent tunneling rates are assumed in Eq. (4) for the sake of simplicity. Inserting Eq. (4) into Eq. (3), we obtain two off-diagonal lesser Green's functions,

$$G_{2,1}^<(t,t)=i\int\frac{d\epsilon}{2\pi}[\Gamma_1 f_1(\epsilon)A_{21}^r(\epsilon,t)A_{11}^a(\epsilon,t)+\Gamma_2 f_2(\epsilon)A_{22}^r(\epsilon,t)A_{21}^a(\epsilon,t)] \tag{5}$$

and

$$G_{1,2}^<(t,t)=i\int\frac{d\epsilon}{2\pi}[\Gamma_2 f_2(\epsilon)A_{12}^r(\epsilon,t)A_{22}^a(\epsilon,t)+\Gamma_1 f_1(\epsilon)A_{11}^r(\epsilon,t)A_{12}^a(\epsilon,t)], \tag{6}$$

as well as two diagonal lesser Green's functions,

$$G_{1,1}^<(t,t)=i\int\frac{d\epsilon}{2\pi}[\Gamma_1 f_1(\epsilon)A_{11}^r(\epsilon,t)A_{11}^a(\epsilon,t)+\Gamma_2 f_2(\epsilon)A_{12}^r(\epsilon,t)A_{21}^a(\epsilon,t)] \tag{7}$$

and

$$G_{2,2}^<(t,t)=i\int\frac{d\epsilon}{2\pi}[\Gamma_2 f_2(\epsilon)A_{22}^r(\epsilon,t)A_{22}^a(\epsilon,t)+\Gamma_1 f_1(\epsilon)A_{21}^r(\epsilon,t)A_{12}^a(\epsilon,t)], \tag{8}$$

where $\int dt_1 e^{i\epsilon(t-t_1)}G_{\ell,j}^r(t,t_1)=A_{\ell,j}^r(\epsilon,t)$ and $\int dt_1 e^{-i\epsilon(t-t_1)}G_{\ell,j}^a(t,t_1)=A_{\ell,j}^a(\epsilon,t)$. The expression of $A_{\ell,j}^{r(a)}(\epsilon,t)$ depends on the detailed form of the retarded and advanced Green's functions. Equations (5) and (6) determine the optical susceptibility of the QDs. Equations (7) and (8) determine the electron occupation numbers. Once $G_{21}^<(t,t)$ is determined, $G_{12}^<(t,t)$ is also obtained as a result of $G_{21}^<(t,t)=[G_{12}^<(t,t)]^\dagger$. To solve $G_{21}^<(t,t)$, some approximations are considered in the following derivation due to the complicated Hamiltonian of Eq. (1). Because the energy level of $\ell=2$ merges into the bandwidth of the left electrode and Γ_2 is larger than Γ_1, the retarded and advanced Green's functions for $\ell=2$ can be regarded as the steady state solution. That is, $G_{22}^{r(a)}(t,t')=\mp i\theta(t-t')e^{-i(\epsilon_2\mp i\Gamma_2/2)(t-t')}$, which gives $A_{22}^{r(a)}\times(\epsilon,t)=1/(\epsilon-\epsilon_2\pm i\Gamma_2/2)$. As for $G_{\ell,j}^{r(a)}(t,t')$, the off-diagonal Green's functions ($\ell\neq j$) are solved using Dyson's equation,

$$G_{\ell,j}^{r(a)}(t,t') = \int dt_1 G_{\ell,\ell}^{r(a)}(t,t_1)\lambda_{\ell,j}G_{j,j}^{r(a)}(t_1,t'). \tag{9}$$

Because $\lambda_{\ell,j} < t_{k,\ell}$ and $G_{\ell,j}^{r(a)}(t,t')$ in terms of the first-order parameter λ, the Green's functions $G_{\ell,\ell}^{r(a)}$ in Eq. (9) are λ-independent functions. Consequently, $A_{21}^{r(a)}(\epsilon,t) = \lambda_{21}A_{22}^{r(a)}(\epsilon)A_{11}^{r(a)}(\epsilon,t)$ and Eq. (5) is rewritten as

$$G_{2,1}^{<}(t,t) = \lambda_{21}\int \frac{d\epsilon}{2\pi}[f_1(\epsilon)\Gamma_1|A_{11}^r(\epsilon,t)|^2 A_{22}^r(\epsilon) + f_2(\epsilon)\Gamma_2|A_{22}^r(\epsilon)|^2 A_{11}^a(\epsilon,t)]. \tag{10}$$

To obtain the spontaneous rate resulting from the imaginary part of $G_{2,1}^{<}(t,t)$, the imaginary part on both sides of Eq. (10) is used:

$$\mathrm{Im}\, G_{2,1}^{<}(t,t) = \lambda_{21}\int \frac{d\epsilon}{2\pi}\Bigg(f_1(\epsilon)\Gamma_1|A_{11}^r(\epsilon,t)|^2 \times\frac{1}{2}[A_{22}^r(\epsilon) - A_{22}^a(\epsilon)] + f_2(\epsilon)\Gamma_2|A_{22}^r(\epsilon)|^2 \times\frac{1}{2}[A_{11}^a(\epsilon,t) - A_{11}^r(\epsilon,t)]\Bigg). \tag{11}$$

Employing $G_\ell^r - G_\ell^a = G_\ell^> - G_\ell^<$, where the greater Green's function is given by

$$G_{\ell,j}^{>}(t,t) = \int dt_1 \int dt_2 G_{\ell,n}^r(t,t_1)\Sigma_{n,m}^{>}(t_1,t_2)G_{m,j}^a(t_2,t) \tag{12}$$

with the greater self-energy

$$\Sigma_{\ell,\ell}^{>}(t,t') = i\int \frac{d\epsilon}{2\pi}\Gamma_\ell(1-f_\ell(\epsilon))e^{-i\epsilon(t-t')}, \tag{13}$$

Eq. (11) can be simplified as

$$\mathrm{Im}\, G_{e,h}^{<}(t,t) = -\lambda_{eh}\int \frac{d\epsilon}{2\pi}\{[1-f_e(\epsilon) - f_h(\epsilon)]\Gamma_h|A_{hh}^r(\epsilon,t)|^2\Gamma_e|A_{ee}^a(\epsilon)|^2\}. \tag{14}$$

In Eq. (14) the electron and hole pictures are employed to label $\ell=2$ and $\ell=1$, respectively. Note that Eq. (14) contains a factor of $[1-f_e(\epsilon)-f_h(\epsilon)]$. It is always possible to write $\lambda_{eh}\mathrm{Im}G_{e,h}^{<}(t,t) = \mathcal{X}_e(\omega,t) - \mathcal{X}_a(\omega,t)$, where $\mathcal{X}_a(\omega,t)$ and $\mathcal{X}_e(\omega,t)$ are, respectively, in proportion to $[1-f_e(\epsilon)][1-f_h(\epsilon)]$ and $f_e(\epsilon)f_h(\epsilon)$. $\mathcal{X}_a(\omega,t)$ and $\mathcal{X}_e(\omega,t)$ denote the absorption and emission spectra, respectively. We focus only on the emission spectrum, which has been frequently reported in experiments,

$$\mathcal{X}_e(\omega,t) = \lambda_{eh}^2\int \frac{d\epsilon}{2\pi}[f_e(\epsilon)f_h(\epsilon)\Gamma_h|A_{hh}^r(\epsilon,t)|^2\Gamma_e|A_{ee}^a(\epsilon)|^2].$$

By reference to Ref. 11, the current arising from the electron-hole recombination of the exciton state may be written as

$$J_{sp}(t) = 2e\alpha\int d\omega\,\omega^3\int \frac{d\epsilon}{\pi^2}f_e(\epsilon)f_h(\epsilon)\Gamma_h|A_{hh}^r(\epsilon,t)|^2\,\mathrm{Im}[A_{ee}^a(\epsilon)] \tag{15}$$

with $\alpha = 4n_r^3\mu_r^2/(6c^3\hbar^3\epsilon_0)$, where n_r and ϵ_0 are the refractive index and static dielectric constant of the system, respectively. e denotes the electron charge. Note that Eq. (15) uses $\Gamma_e|A_{ee}^a(\epsilon)|^2 = 2\mathrm{Im}[A_{ee}^a(\epsilon)]$ which is valid only for the steady state. $\rho(\omega)=\omega^2$ of Eq. (15) arises from the density of states of photons. $J_{sp}(t)$ is determined by the time-dependent interband joint density of states and the factors of $f_e(\epsilon)f_h(\epsilon)$. According to the expressions for $\mathcal{X}_e(\omega,t)$ and $J_{sp}(t)$, we prove that the intensity of the emission exciton spectrum varies linearly with respect to $J_{sp}(t)$.[3]

To solve the spectral function of the holes $A_{hh}^r(\epsilon,t)$, the retarded Green's function of holes $G_{hh}^r(t,t_1)$ is derived to obtain

$$G_{hh}^r(t,t_1) = (1-N_e)g_h^r(\epsilon_h,t,t_1) + N_e g_h^r(\epsilon_h+U_{eh},t,t_1) \tag{16}$$

with

$$g_h^r(\epsilon_h,t,t_1) = -i\theta(t-t_1)\times\exp\Bigg(-i(\epsilon_h - i\Gamma_h/2)(t-t_1) - i\int_{t_1}^{t} dt_2 v(t_2)\Bigg), \tag{17}$$

where $\epsilon_h = -E_h + \omega/2$, and N_e is the electron occupation number at steady state. Two branches exist in Eq. (16); one corresponds to the resonant energy level of E_h with a weight of $(1-N_e)$, and the other corresponds to the exciton resonant level of $E_{ex}=E_h-U_{eh}$ with a weight of N_e. Consequently, holes injected into the energy levels of QDs depend not only on the applied voltage of the right electrode, but also on the electron occupation number N_e, which is given by $N_e = \int(d\epsilon/\pi)f_e(\epsilon)\mathrm{Im}[1/(\epsilon - E_e - i\Gamma_e/2)]$. Because $N_e=1$, it is only necessary to consider the exciton branch of $g_h^r(\epsilon_h + U_{eh},t,t_1)$ in Eq. (16). The detailed expression of $G_{hh}^r(t,t_1)$ depends on the applied voltage $v(t)$, considering a rectangular pulse with the duration time of Δs and amplitude Δ as $v(t)$. For $0 \leqslant t < \Delta s$, according to Eq. (17),

$$A_{hh}^r(\epsilon,t) = \frac{1}{\epsilon - \epsilon_h + i\Gamma_h/2}\Bigg(1 + \frac{\Delta}{\epsilon - \epsilon_h - \Delta + i\Gamma_h/2}\times(1 - e^{i(\epsilon-\epsilon_h-\Delta+i\Gamma_h/2)t})\Bigg). \tag{18}$$

For $t \geqslant \Delta s$,

$$A_{hh}^r(\epsilon,t) = \frac{1}{\epsilon - \epsilon_h - \Delta + i\Gamma_h/2}\Bigg(1 + \frac{\Delta}{\epsilon - \epsilon_h + i\Gamma_h/2}\times(1 - e^{i(\epsilon-\epsilon_h+i\Gamma_h/2)(t-\Delta s)})(1 - e^{i(\epsilon-\epsilon_h-\Delta+i\Gamma_h/2)\Delta s})\Bigg). \tag{19}$$

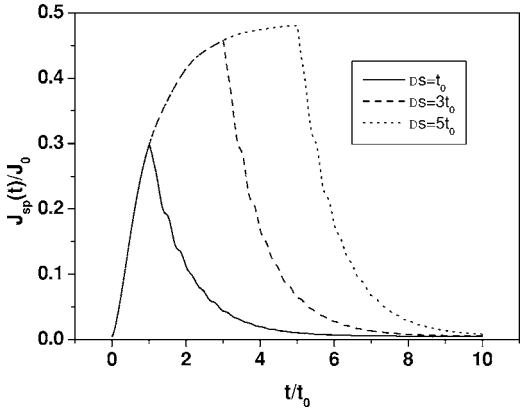

FIG. 2. Time-dependent current arising from the electron-hole recombination $J_{sp}(t)$ for different duration times of applied rectangular pulse voltage with amplitude $\Delta=20$ meV at zero temperature. Current is given in units of $J_0=2eR_{eh}$, where R_{eh} denotes the time- and temperature-independent spontaneous emission rate, and time is in units of $t_0=\hbar/\text{meV}$.

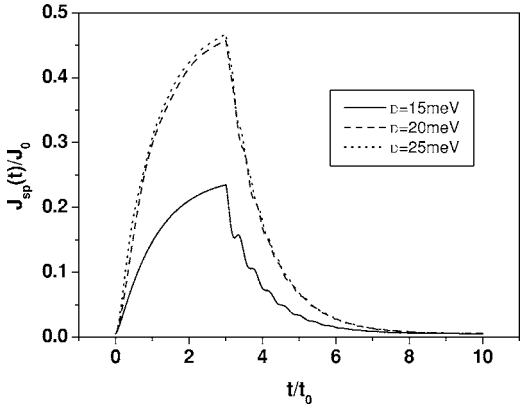

FIG. 3. Time-dependent current arising from the electron-hole recombination $J_{sp}(t)$ for different applied voltages with duration time $\Delta s=3t_0$ at zero temperature. Current is given in units of $J_0=2eR_{eh}$, where R_{eh} denotes the time- and temperature-independent spontaneous emission rate, and time is in units of $t_0=\hbar/\text{meV}$.

The time-dependent tunneling current associated with the spontaneous radiative transition in individual quantum dots is next discussed based on Eqs. (15), (18), and (19).

IV. RESULTS AND DISCUSSION

Because of current conservation, the time-dependent tunneling current is given by $J(t)=J_{sp}(t)=e\Gamma_s(t)$, where $\Gamma_s(t)$ denotes the time-dependent spontaneous emission rate. Owing to small tunneling rates ($\Gamma_e/E_{F,e}\ll 1$ and $\Gamma_h/E_{F,h}\ll 1$), Eq. (15) can be reduced to

$$J_{sp}(t)=2eR_{eh}f_e(T)N_h(T,t), \tag{20}$$

with

$$N_h(t)=\int \frac{d\epsilon}{\pi} f_h(\epsilon)\Gamma_h|A^r_{hh}(\epsilon,t)|^2. \tag{21}$$

We note that $A^r_{hh}(\epsilon,t)$ satisfies the condition of $\Gamma_h|A^r_{hh}(\epsilon,t)|^2=-2\,\text{Im}[A^r_{hh}(\epsilon,t)]-d|A^r_{hh}(\epsilon,t)|^2/dt$ resulting from total charge conservation and gauge invariance.[16] In Eq. (20) we define the time-independent spontaneous emission rate $R_{eh}=\alpha\Omega^3_{ex}$, where $\Omega_{ex}=E_g+E_e+E_h-U_{eh}$. According to Eq. (20), the time-dependent feature of $J_{sp}(t)$ is determined by the hole occupation number of Eq. (21).

To reveal the time-dependent behavior of $J_{sp}(t)$, Eq. (20) is solved numerically, and shows $J_{sp}(t)$ for various duration times at zero temperature in Fig. 2 for the tunneling rate $\Gamma_h=0.5$ meV and $\Delta=20$ meV; the solid line for $\Delta s=t_0$, the dashed line for $\Delta s=3t_0$, and the dotted line for $\Delta s=5t_0$. The current almost reaches saturation at $t=5t_0$. Apart from the classical capacitive charging and discharging behavior (exponential growth and decay),[17] tunneling oscillations are superimposed on the tunneling current not only for $t\leqslant\Delta s$ but also for $t>\Delta s$. However, the amplitude of oscillation for $t\leqslant\Delta s$ is small. In particular, the oscillation period for $t>\Delta s$ does not depend on the magnitude of the duration time. The oscillatory current is given by the particle coherent tunneling between the electrodes and the QD. Such coherent tunneling was also pointed out as the mechanism of quantum ringing for the electron tunneling current through a single dot embedded in an *n-i-n* structure.[18] In Ref. 18 oscillatory current was not observed as $t>\Delta s$. According to the result of quantum interference between the outgoing wave (leaving the QDs) and the wave reflected from the barrier, this oscillatory behavior could be observed in the discharging process.[19]

To examine if the oscillation currents shown in Fig. 2 depend on the applied bias strength, Fig. 3 illustrates $J_{sp}(t)$ for different applied biases with duration time $\Delta s=3t_0$ at zero temperature and $\Gamma_h=0.5$ meV. The solid line denotes $\Delta=15$ meV, and the dashed and dotted lines denote $\Delta=20$ and 25 meV, respectively. For amplitude $\Delta=15$ meV, the Fermi energy of the right electrode just reaches alignment with the resonant exciton level. $J_{sp}(t)$ displays a strong oscillation characteristic. If the pulse amplitude is increased to $\Delta=20$ meV, the resonant exciton level is covered by the right electrode reservoir, and therefore the magnitude of $J_{sp}(t)$ increases. When the pulse amplitude is increased to $\Delta=25$ meV, $J_{sp}(t)$ becomes saturated. The results shown in Fig. 3 clearly indicate that the oscillation feature of $J_{sp}(t)$ depends on the magnitude of Δ. Because the number of emitted photons is in proportion to $J_{sp}(t)$, the features of the emitted photon numbers as functions of time will correspond to the results shown in Fig. 3.

In Figs. 2 and 3 the hole tunneling rate is set as $\Gamma_h=0.5$ meV; it is interesting to understand how the tunneling rate influences $J_{sp}(t)$. $J_{sp}(t)$ for different hole tunneling rates is shown in Fig. 4; the solid line for $\Gamma_h=0.5$ meV, the dashed line for $\Gamma_h=0.75$ meV, and the dotted line for $\Gamma_h=1$ meV. On increasing the tunneling rate, $J_{sp}(t)$ reaches exponential growth quickly. This also indicates that electrically driven SPSs can quickly reach the maximum photon emission efficiency within a shorter operating time compared to optically driven SPSs with a phonon bottleneck. To clarify, the relation between the photon number $N_s(t)$ and $J_{sp}(t)$ should be constructed. Because $dN_s(t)/dt=\Gamma_{sp}(t)$, the time-dependent photon number $N_s(t)=\int_0^t dt\,\Gamma_{sp}(t)$ is obtained. For a steplike

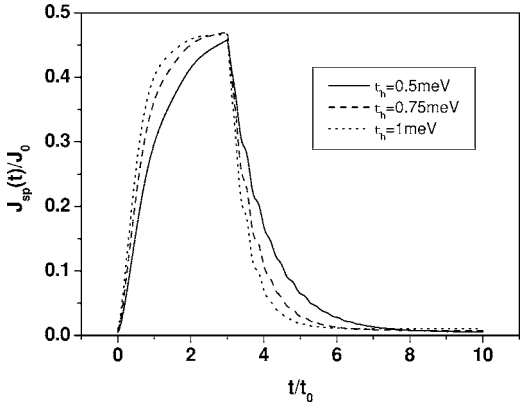

FIG. 4. Time-dependent current arising from the electron-hole recombination $J_{sp}(t)$ for different tunneling rates of holes at zero temperature and the applied voltage with duration time $\Delta s=3t_0$ and amplitude $\Delta=20$ meV. Current is given in units of $J_0=2eR_{eh}$, where R_{eh} denotes the time- and temperature-independent spontaneous emission rate, and time is in units of $t_0=\hbar/\mathrm{meV}$.

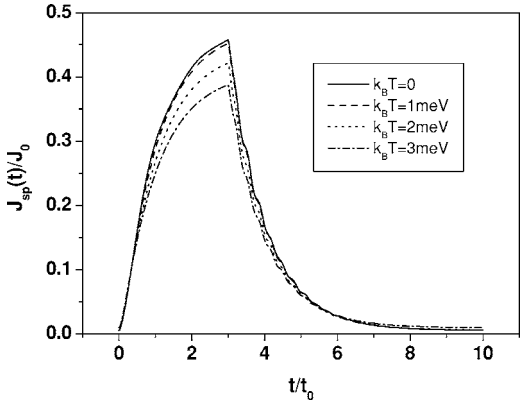

FIG. 5. Time-dependent current arising from the electron-hole recombination $J_{sp}(t)$ for different temperatures at the applied voltage with duration time $\Delta s=3t_0$ and amplitude $\Delta=20$ meV. Current is given in units of $J_0=2eR_{eh}$, where R_{eh} denotes the time- and temperature-independent spontaneous emission rate, and time is in units of $t_0=\hbar/\mathrm{meV}$.

pulse ($\Delta s=\infty$), $A^r_{hh}(\epsilon,t)$ is given by Eq. (18). Due to the small oscillatory amplitude in the charging process, Eq. (21) is approximated as $N_h(t)=f_h(T)(1-e^{-\Gamma_h t})$ for $t\geqslant 0$. Consequently, $N_s(t)=R_{eh}f_e(T)f_h(T)t[1+(e^{-\Gamma_h t}-1)/(\Gamma_h t)]$. We found that $N_s(t)/t=R_{eh}f_e(T)f_h(T)$ as $\Gamma_h t\gg 1$. This indicates that a higher tunneling rate allows an electrically driven SPS to quickly reach the maximum photon emission efficiency.

Finally, the finite-temperature effect on $J_{sp}(t)$ is shown in Fig. 5; the solid line is for $k_BT=0$, the dashed line for $k_BT=1$ meV, the dotted line for $k_BT=2$ meV, and the dot-dashed line for $k_BT=3$ meV. Figure 5 shows that the spontaneous photon emission rate $\Gamma_{sp}(t)$ is suppressed by temperature effects resulting from the factor of $f_e(T)f_h(T)$. From Fig. 2 to Fig. 5, $J_{sp}(t)$ is in units of $J_0=2eR_{eh}$. For InAs QDs, the typical value of R_{eh} is on the order of 1 μeV/ns.[20] This indicates that J_{sp} results from spontaneous photon emission on the order of nanoamperes, which can be readily measured.

V. SUMMARY

The expression for the tunneling current $J_{sp}(t)$ arising from spontaneous radiative transition in individual quantum dots is obtained by using the nonequilibrium Green's function method. $J_{sp}(t)$ is found to be a function of the spontaneous emission rate R_{eh}, the tunnelling rates Γ_h (Γ_e), and the factor of $f_e(T)f_h(T)$. In addition to the exponential growth and decay features corresponding to the charging and discharging processes, oscillatory behavior of $J_{sp}(t)$ as a function of time is observed as a result of particle coherent tunneling between the electrodes and QDs, which is suppressed by the temperature effects.

In this study, resonant tunneling carriers are used to yield triggered single-photon sources, in contrast to the captured carriers typically used in an optically driven SPS.[21,22] Due to the phonon bottleneck effect,[23] it is predicted that the QD capture rate of electrons will be low. This could reduce the performance of SPS devices, which use captured carriers as the source of single-photon generations. Using carriers injected via the resonant tunneling process can prevent such problems.

ACKNOWLEDGMENTS

This work was supported by National Science Council of the Republic of China Contracts No. NSC 94-2215-E-008-027 and No. NSC 94-2120-M-008-002.

[1] O. Benson, C. Santori, M. Pelton, and Y. Yamamoto, Phys. Rev. Lett. **84**, 2513 (2000).
[2] P. Michler, A. Kiraz, C. Becher, W. V. Schoenfeld, P. M. Petroff, L. D. Zhang, E. Hu, and A. Imamoglu, Science **290**, 2282 (2000).
[3] Z. L. Yuan, B. E. Kardynal, R. M. Stevenson, A. J. Shield, C. J. Lobo, K. Cooper, N. S. Beattlie, D. A. Ritchie, and M. Pepper, Science **295**, 102 (2002).
[4] A. Imamoglu and Y. Yamamoto, Phys. Rev. Lett. **72**, 210 (1994).
[5] C. K. Hahn, J. Motohisa, and T. Fukui, Appl. Phys. Lett. **76**, 3947 (2000).
[6] H. Cao, G. Klimovitch, G. Bjork, and Y. Yamamoto, Phys. Rev. B **52**, 12184 (1995).
[7] Y. N. Chen and D. S. Chuu, Phys. Rev. B **66**, 165316 (2002).
[8] David M.-T. Kuo and Y. C. Chang, Phys. Rev. B **72**, 085334 (2005).
[9] H. Haug and A. P. Jauho, *Quantum Kinetics in Transport and Optics of Semiconductors* (Springer, Heidelberg, 1996).
[10] A. P. Jauho, N. S. Wingreen, and Y. Meir, Phys. Rev. B **50**, 5528 (1994).

[11] H. Haug and S. W. Koch, *Quantum Theory of the Optical and Electronic Properties of Semiconductors* (World Scientific, Singapore, 1990).
[12] R. Aguado, J. Inarrea, and G. Platero, Phys. Rev. B **53**, 10030 (1996).
[13] Q. F. Sun, J. Wang, and T. H. Lin, Phys. Rev. B **61**, 12643 (2000).
[14] J. Merino and J. B. Marston, Phys. Rev. B **69**, 115304 (2004).
[15] G. Stefanucci and C. O. Almbladh, Phys. Rev. B **69**, 195318 (2004).
[16] B. Wang, J. Wang, and H. Guo, Phys. Rev. Lett. **82**, 398 (1999).
[17] J. Q. You, C. H. Lam, and H. Z. Zheng, Phys. Rev. B **62**, 1978 (2000).
[18] N. S. Wingreen, A. P. Jauho, and Y. Meir, Phys. Rev. B **48**, 8487 (1993).
[19] David M.-T. Kuo and Y. C. Chang, Phys. Rev. B **60**, 15957 (1999).
[20] G. S. Solomon, M. Pelton, and Y. Yamamoto, Phys. Rev. Lett. **86**, 3903 (2001).
[21] W. H. Chang, W. Y. Chen, H. S. Chang, T. P. Hsieh, J. I. Chyi, and T. M. Hsu, Phys. Rev. Lett. **96**, 117401 (2006).
[22] D. Englund, D. Fattal, E. Waks, G. Solomon, B. Zhang, T. Nakaoka, Y. Arakawa, Y. Yamamoto, and J. Vuckovic, Phys. Rev. Lett. **95**, 013904 (2005).
[23] J. Urayama, T. B. Norris, J. Singh, and P. Bhattacharya, Phys. Rev. Lett. **86**, 4930 (2001).